nature microbiology

ARTICLES

PUBLISHED: 17 OCTOBER 2016 | VOLUME: 2 | ARTICLE NUMBER: 16188

Helicobacter pylori exploits human CEACAMs via HopQ for adherence and translocation of CagA

Verena Königer[1†], Lea Holsten[1†], Ute Harrison[1], Benjamin Busch[1], Eva Loell[1], Qing Zhao[1], Daniel A. Bonsor[2], Alexandra Roth[3], Arnaud Kengmo-Tchoupa[3], Stella I. Smith[4], Susanna Mueller[5], Eric J. Sundberg[2,6,7], Wolfgang Zimmermann[8,9], Wolfgang Fischer[1], Christof R. Hauck[3] and Rainer Haas[1,10]*

***Helicobacter pylori* (*Hp*) strains that carry the *cag* type IV secretion system (*cag*-T4SS) to inject the cytotoxin-associated antigen A (CagA) into host cells are associated with peptic ulcer disease and gastric adenocarcinoma. CagA translocation by *Hp* is mediated by β1 integrin interaction of the *cag*-T4SS. However, other cellular receptors or bacterial outer membrane adhesins essential for this process are unknown. Here, we identify the HopQ protein as a genuine *Hp* adhesin, exploiting defined members of the carcinoembryonic antigen-related cell adhesion molecule family (CEACAMs) as host cell receptors. HopQ binds the amino-terminal IgV-like domain of human CEACAM1, CEACAM3, CEACAM5 or CEACAM6 proteins, thereby enabling translocation of the major pathogenicity factor CagA into host cells. The HopQ–CEACAM interaction is characterized by a remarkably high affinity (K_D from 23 to 268 nM), which is independent of CEACAM glycosylation, identifying CEACAMs as bona fide protein receptors for *Hp*. Our data suggest that the HopQ–CEACAM interaction contributes to gastric colonization or *Hp*-induced pathologies, although the precise role and functional consequences of this interaction *in vivo* remain to be determined.**

The highly motile, microaerophilic, Gram-negative bacterium, *Heliobacter pylori*, infects the gastric mucus layer of about half the human population. This infection is a major cause of gastroduodenal disease, including chronic active gastritis, peptic ulcer disease, mucosa-associated lymphoid tissue (MALT) lymphoma and gastric adenocarcinoma[1,2]. The 37 kb *cag*-pathogenicity island (*cag*-PAI) encodes the cytotoxin-associated gene A (CagA), as well as the *cag* type IV secretion system (*cag*-T4SS), which forms a membrane-spanning secretion channel and an extracellular pilus. On contact with target cell receptors such as the $\alpha_5\beta_1$ integrin heterodimer[3,4], the effector protein CagA is translocated into host cells[5] and secretion of the proinflammatory chemokine interleukin-8 (IL-8) is induced[6,7]. Injected CagA is tyrosine-phosphorylated on multiple Glu-Pro-Ile-Tyr-Ala (EPIYA) motifs in the C-terminal region of the CagA protein, which enables CagA to interact with a large repertoire of cellular target proteins[8–10]. CagA may disrupt tight junctions and cause the loss of epithelial cell polarity[11,12]. Due to its correlation with the risk of cancer development in humans[13] and its role in pathogenesis in mouse and Mongolian gerbil infection models[14,15], CagA is considered a bacterial oncoprotein[16]. Several outer membrane proteins (OMPs) of *Hp* have been identified recently as functional contributors to the *cag*-T4SS. BabA-mediated adherence of *Hp* acts as a potentiator of *cag*-T4SS activity[17], whereas HopQ was found to be crucial for translocation of CagA via the *cag*-T4SS (ref. 18), but also to restrict CagA translocation for a subsequent *Hp* strain into the same host cell[19]. These data suggest that, besides β_1 integrin, other host cell receptors might be exploited by *Hp* for binding and CagA injection.

The carcinoembryonic antigen-related cell adhesion molecules (CEACAMs) are a diverse group of cell surface glycoproteins that are part of the immunoglobulin (Ig) superfamily. CEACAMs are involved in cell–cell recognition and modulate cellular processes ranging from the shaping of tissue architecture and neovascularization to the regulation of insulin homeostasis and T-cell proliferation[20,21]. A number of human-specific Gram-negative bacteria specifically adhere to CEACAMs[22]. Here, we report that *Hp* also exploits CEACAMs to bind to host cells and to inject its major virulence factor, the CagA oncoprotein, into mammalian cells.

Results

Specific binding of *Hp* to IgV-like domains of human CEACAM1 and CEACAM5. CEACAMs are expressed on the apical surface of epithelial cells, and several human-specific Gram-negative pathogens are known to exploit CEACAMs to infect their host[23]. To assess the potential interactions between *Hp*, which also specifically infects humans, and CEACAMs, we incubated soluble CEACAM–green fluorescent protein (GFP) fusion proteins (designated as CEA1–CEA8-N-GFP, Fig. 1a,b) with *Hp* strain P12 (ref. 24). Centrifugation of intact bacteria pulled down CEA1-N-GFP and CEA5-N-GFP, as detected by immunoblotting with an

[1]Max von Pettenkofer-Institut für Hygiene und Medizinische Mikrobiologie, Ludwig-Maximilians-Universität, Pettenkoferstraße 9a, D-80336 München, Germany. [2]Institute of Human Virology, University of Maryland School of Medicine, University of Maryland, Baltimore, Maryland 21201, USA. [3]Lehrstuhl Zellbiologie, Fachbereich Biologie, Universität Konstanz, D-78457 Konstanz Germany. [4]Molecular Biology and Biotechnology Division, Nigerian Institute of Medical Research, 6 Edmond Crescent, Yaba, PMB 2013 Lagos, Nigeria. [5]Institut für Pathologie, Ludwig-Maximilians-Universität, D-80337 München, Germany. [6]Department of Medicine, University of Maryland School of Medicine, University of Maryland, Baltimore, Maryland 21201, USA. [7]Department of Microbiology and Immunology, University of Maryland School of Medicine, University of Maryland, Baltimore, Maryland 21201, USA. [8]Tumor Immunology Laboratory, LIFE Center, Ludwig-Maximilians-Universität, Feodor-Lynen-Str. 19, D-81377 München, Germany. [9]Department of Urology, University Hospital, Ludwig-Maximilians-Universität, Marchioninistr. 15, D-81377 München, Germany. [10]German Center for Infection Research (DZIF), partner site LMU München, Germany. †These authors contributed equally to this work. *e-mail: r.haas@lmu.de

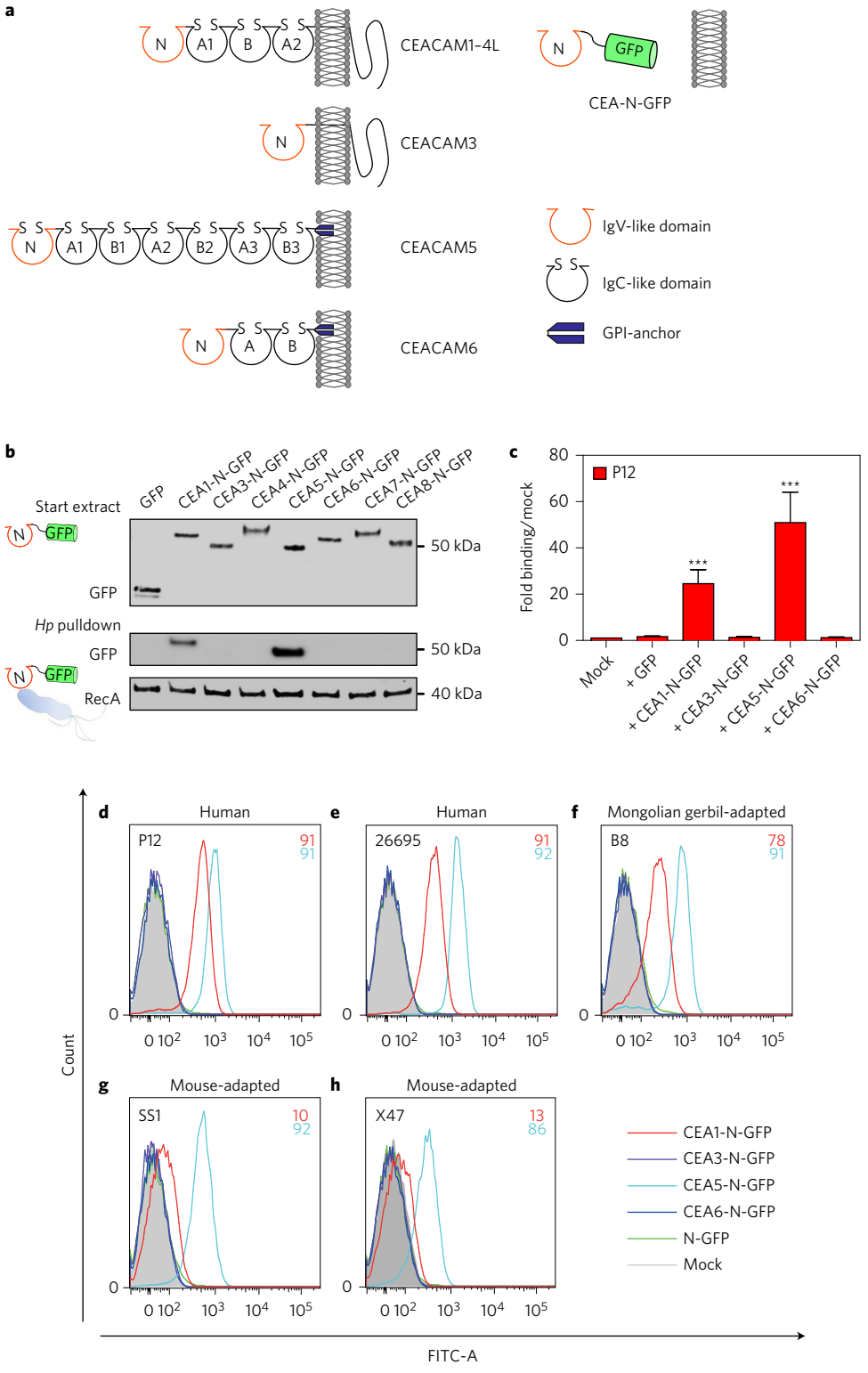

Figure 1 | *Hp* interacts with soluble CEACAM1 and CEACAM5 molecules with different specificities. a, The human CEACAM1-4L and CEACAM3 proteins contain a transmembrane and a cytoplasmic domain, whereas CEACAM5 and CEACAM6 insert via glycosylphosphatidylinositol (GPI) anchors into the membrane. For pulldown assays, soluble N-terminal IgV-like domains of different CEACAMs fused to GFP were used (CEA-N-GFP). **b**, Bacterial pulldown assays using culture supernatants of transiently transfected HEK293 cells and *Hp* were performed as described in the Methods using an anti-GFP antibody for immunoblotting. Anti-RecA was used for bacterial normalization. This is a representative gel of an experiment that was performed three times. **c**, Culture supernatants containing soluble CEA-N-GFP proteins or control supernatant (GFP-transfected cells) were incubated with *Hp* P12 bacteria. After extensive washing, bacteria were analysed by flow cytometry and bacteria-associated GFP was determined. **d**–**h**, Various *Hp* strains (human, gerbil-adapted, mouse-adapted) were incubated with CEA-N-GFP culture supernatants and analysed by flow cytometry. Percentage of the population shifted is indicated at the top right corner for CEACAM1 (red) and CEACAM5 (blue). Representative plots are shown of experiments that were performed three times. For **c**, Student's *t*-test, one-tailed; $^{***}P < 0.001$. Values are means ± s.e.m.

anti-GFP antibody (Fig. 1b). Flow cytometry measurements verified the binding of CEA1-N-GFP and CEA5-N-GFP (Fig. 1c), but none of the other CEA-N-GFP constructs, as ligands for *Hp* (Supplementary Fig. 1a). Pulldown of CEA5-N-GFP by P12 was significantly stronger (4.3-fold) than of CEA1-N-GFP (Supplementary Fig. 1b). A similar binding pattern was observed for the CEACAM-binding reference strain *Moraxella catarrhalis* ATCC25238 (Supplementary Fig. 1c) and for additional *Hp* strains (Supplementary Fig. 1d). Thus, *Hp* binds specifically to soluble N-terminal domains of human CEACAM1 and CEACAM5.

From this set of independent *Hp* strains, three (P12, 26695 and the Mongolian gerbil-adapted strain B8) interacted with CEA1-N-GFP and even more strongly with CEA5-N-GFP, but not with any other CEA-N-GFP protein tested (Fig. 1d–f). In contrast, the mouse-adapted strains SS1 and X47 revealed a moderate to strong binding to CEACAM5, but only weak binding to CEACAM1 (Fig. 1g,h). Interestingly, none of the non-human CEA1-N-GFP (murine, bovine or canine) or CEA5-N-GFP (macaque) fusion proteins reacted with the above set of *Hp* strains (Supplementary Fig. 2a). These results indicate that the association of *Hp* with CEACAM1 and CEACAM5 and its intensity varies between strains, but is highly specific for the human receptors.

HopQ is the *Hp* adhesin binding CEACAM1 and CEACAM5 N-terminal domains. *Hp* produces a large number of OMPs, including the *Helicobacter* outer protein (Hop) and Hop-related (Hor) gene families, which are differently present or expressed in independent *Hp* strains. A phylogenetic tree generated from the Hop and Hor protein families revealed that most of the known *Hp* adhesins (BabA, BabB, BabC, SabA, HopD and HopZ) clustered together in an isolated branch (Supplementary Fig. 2b). *Hp babA*, *babB*, *sabB* or *hopZ* mutants did not differ significantly in soluble CEA1-N-GFP and CEA5-N-GFP binding from wild type (wt) P12 (Supplementary Fig. 2c). By generating additional mutant strains within this putative 'adhesin family' (Supplementary Table 1), we identified *hopQ* deletion mutants as defective in the binding of CEA1-N-GFP or CEA5-N-GFP (Fig. 2a). Genetic complementation using the plasmid-based pHel shuttle vector system[25] completely restored the CEACAM-binding capacity of this mutant strain (Fig. 2a). Using a peptide-based antiserum (AK298) directed against the HopQ type I-specific protein region, we verified the production of HopQ in the corresponding strains (Fig. 2b). HopQ I proteins are typically associated with *Hp* strains carrying a functional *cag*-T4SS, whereas T4SS-negative *Hp* strains often produce a HopQ II protein[26] that differs markedly from HopQ I and is not recognized by AK298 (Fig. 2b and Supplementary Fig. 3). In the genetically complemented P12Δ*hopQ*::*hopQ* I strain, HopQ I is overproduced relative to P12 (Fig. 2b), explaining the stronger relative binding to CEACAM1 and CEACAM5 (Fig. 2a). Together, these data show that *Hp* uses HopQ to bind the CEACAM1 and CEACAM5 N-terminal domains.

HopQ binding of non-glycosylated N-terminal CEACAM domains with high affinity. To determine whether HopQ and CEACAMs interact directly, we produced HopQ as a maltose binding protein (MBP) fusion (Supplementary Table 2). The N-terminal domains of CEACAM1, CEACAM3, CEACAM5 and CEACAM8 (CEA-N) were produced in *Escherichia coli* (Supplementary Fig. 4a) and their affinity for HopQ was measured by isothermal titration calorimetry (ITC). MBP–HopQ, but not MBP alone (Supplementary Fig. 4b), bound with high affinity to CEA1-N ($K_D = 23 \pm 1$ nM) and to CEA5-N ($K_D = 61 \pm 3$ nM), with lower affinity to CEA3-N ($K_D = 268 \pm 4$ nM), but did not show binding to CEA8-N (Fig. 2c–f) (Supplementary Table 3). The stoichiometry was determined as one MBP–HopQ to half of a CEA-N dimer (1:0.62), similar to other bacterial adhesin–CEACAM5 interactions[27]. Corroborating our bacterial pulldown assays, these data clearly demonstrate that *Hp* uses its OMP HopQ as an adhesin to interact directly and with high affinity, with the N-terminal domain of defined CEACAM proteins, even in the absence of CEA-N glycosylation. Thus, the HopQ–CEACAM interaction is the first protein–protein adhesin-receptor interaction described for *Hp*.

Surface localization of CEACAMs on epithelial cell lines correlates with CagA translocation by *Hp*. We have previously shown that a P12Δ*hopQ* mutant strain is severely impaired in its capacity to translocate CagA into gastric epithelial cells[18]. By flow cytometry analysis, we observed CEACAM1, CEACAM5 and CEACAM6 expression on the surface of AGS, Kato III and MKN45 cells, but not on MKN28, HeLa or HEK293 cells (Fig. 3a). None of this latter set of cells, producing little or no CEACAMs on their surface, was permissive for CagA translocation. In contrast, AGS, Kato III and MKN45 cells, all of which produce significant amounts of these CEACAMs, were competent for translocation of CagA. Notably, MKN45 cells, producing significantly more CEACAM5 and CEACAM6 than the other cell lines, exhibited the strongest capacity for CagA translocation by *Hp* (Fig. 3a). These data point to a correlation between CEACAM1, CEACAM5 and CEACAM6 cell surface presentation and the ability of *Hp* P12 to translocate CagA.

HopQ-specific adhesion and CagA translocation in HEK293 cells. To determine whether the absence of cell surface expression of CEACAMs is responsible for a defect in CagA translocation, stably CEACAM1- or CEACAM5-transfected HEK293 cells (Supplementary Table 4) were analysed for proper CEACAM production and surface localization by flow cytometry. *Hp* infection of these cells resulted in efficient CagA translocation (Fig. 3b,c), demonstrating that CagA translocation can be completely restored by adding a single receptor for the *Hp* OMP HopQ, either CEACAM1 or CEACAM5.

We next developed a flow cytometry-based quantitative binding assay using the GFP-labelled *Hp* P12 strain and stably transfected HEK293 cells producing the N-terminal (CEACAM5ΔIgC) or constant domains of CEACAM5 (CEACAM5ΔIgV) (Fig. 4a). HEK293 cells, producing CEACAM5ΔIgC, showed a significant HopQ-dependent adherence (Fig. 4b) and CagA translocation (Fig. 4c), whereas CEACAM5ΔIgV-producing cells did not. Thus, the presence of the N-terminal domain of CEACAM5 on host cells is necessary and sufficient to support both *Hp* adherence and CagA translocation into HEK293 cells *in vitro*.

The amino-acid sequences of the N-terminal domains of human CEACAMs are well conserved between CEACAM1, CEACAM3, CEACAM5 or CEACAM6, whereas CEACAM4 and CEACAM8 diverge substantially (Supplementary Fig. 4c). Transient transfection of HEK293 cells with expression plasmids encoding these additional CEACAMs resulted in CEACAM surface localization (Fig. 4e, bottom). Notably, for CEACAM3- and CEACAM6-, but not for CEACAM4- or CEACAM8-producing cells, we observed specific binding of *Hp* (Fig. 4d), as well as CagA translocation (Fig. 4e, top). The binding of *Hp* to cell surface-exposed CEACAM3 and CEACAM6 was in contrast to our results obtained with soluble CEA3-N-GFP and CEA6-N-GFP, which did not show binding (Fig. 1c), but is supported by the ITC data (Fig. 2c–f). Thus, membrane localization and potential clustering of these receptors may provide better accessibility of binding epitopes for HopQ as compared to the constructs.

A specific siRNA knockdown of CEACAM1, CEACAM5 and CEACAM6 in AGS cells was up to 100% for CEACAM1, 70% for CEACAM5 and 73% for CEACAM6 (Supplementary Fig. 5a).

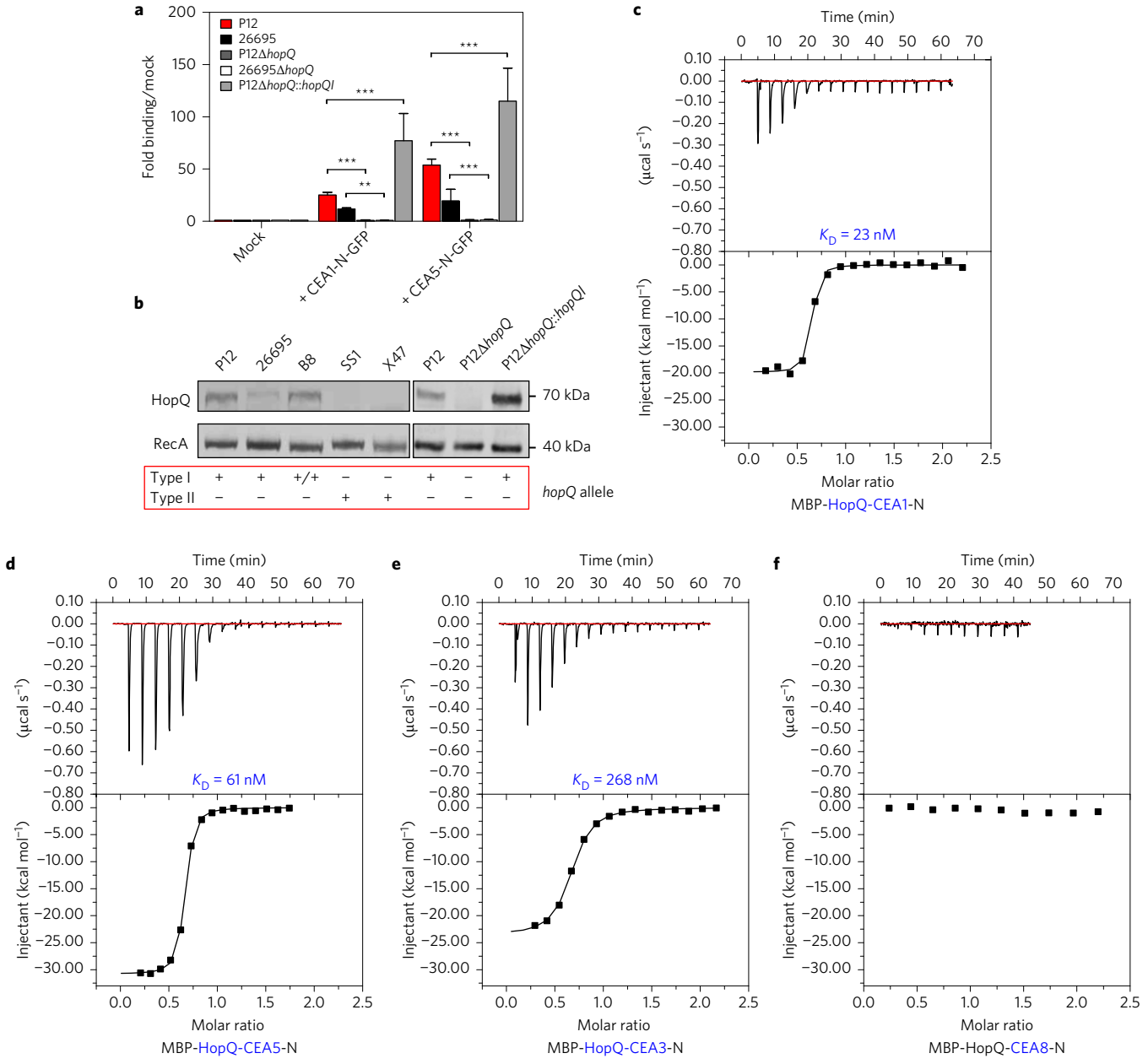

Figure 2 | The *Hp* outer membrane protein HopQ is the adhesin interacting with soluble CEACAM1 and CEACAM5. a, *Hp* P12 and 26695 WT, isogenic *hopQ* mutant strains and a complemented P12Δ*hopQ* mutant were used for the bacterial pulldown assay and measured by flow cytometry. **b**, Immunoblots showing HopQ production by different *Hp* strains and their *hopQ* alleles. The rabbit α-HopQ I peptide antibody (AK298) specifically recognizes HopQ I, but not HopQ II. This is a representative blot of an experiment that was performed twice. **c**–**f**, Isothermal titration calorimetry (ITC) binding curves of different CEACAM N-terminal IgV-like domains (CEA-N) titrated against MBP-HopQ. K_D values are indicated next to the curves. These are representative titration curves of an experiment that was performed three times. For **a**, Student's *t*-test, for *hopQ* mutant two-tailed, other strains one-tailed; $^{**}P < 0.01$, $^{***}P < 0.001$. Values are means ± s.e.m.

Knockdown of individual CEACAMs did not show a significant inhibition of CagA translocation, suggesting a functional redundancy. However, the simultaneous knockdown of all three CEACAMs reduced CagA translocation to a level comparable to that observed for the *Hp* P12Δ*hopQ* mutant on AGS cells (Supplementary Fig. 5a,b). These observations suggest that AGS cells express at least one additional unknown receptor recognized by an unknown *Hp* adhesin, which supports CagA translocation and seems to be absent in HEK293 cells (Supplementary Fig. 5a,b).

Correlation of *Hp* adherence, HopQ-mediated recruitment of CEACAM5 and CagA injection. To study the functional relevance of the HopQ–CEACAM interaction for CagA translocation, we performed confocal laser scanning microscopy (CLSM) using different human gastric epithelial cell lines, AGS, MKN45 and Kato III. Infection resulted in a strong adherence and co-localization of *Hp* P12 WT and the genetically complemented *hopQ* mutant (P12Δ*hopQ*::*hopQ I*) with CEACAM5 on the cell surface (Supplementary Fig. 6a–c, yellow arrows). In the absence of HopQ (P12Δ*hopQ*), co-localization of *Hp* with CEACAM5 was not observed on any of the tested cells (Supplementary Fig. 6, arrowheads). However, in the P12Δ*hopQ* strain, *Hp* binding to AGS cells was only slightly reduced (statistically not significant), but almost abolished for MKN45 cells (Supplementary Fig. 6a,b,d,

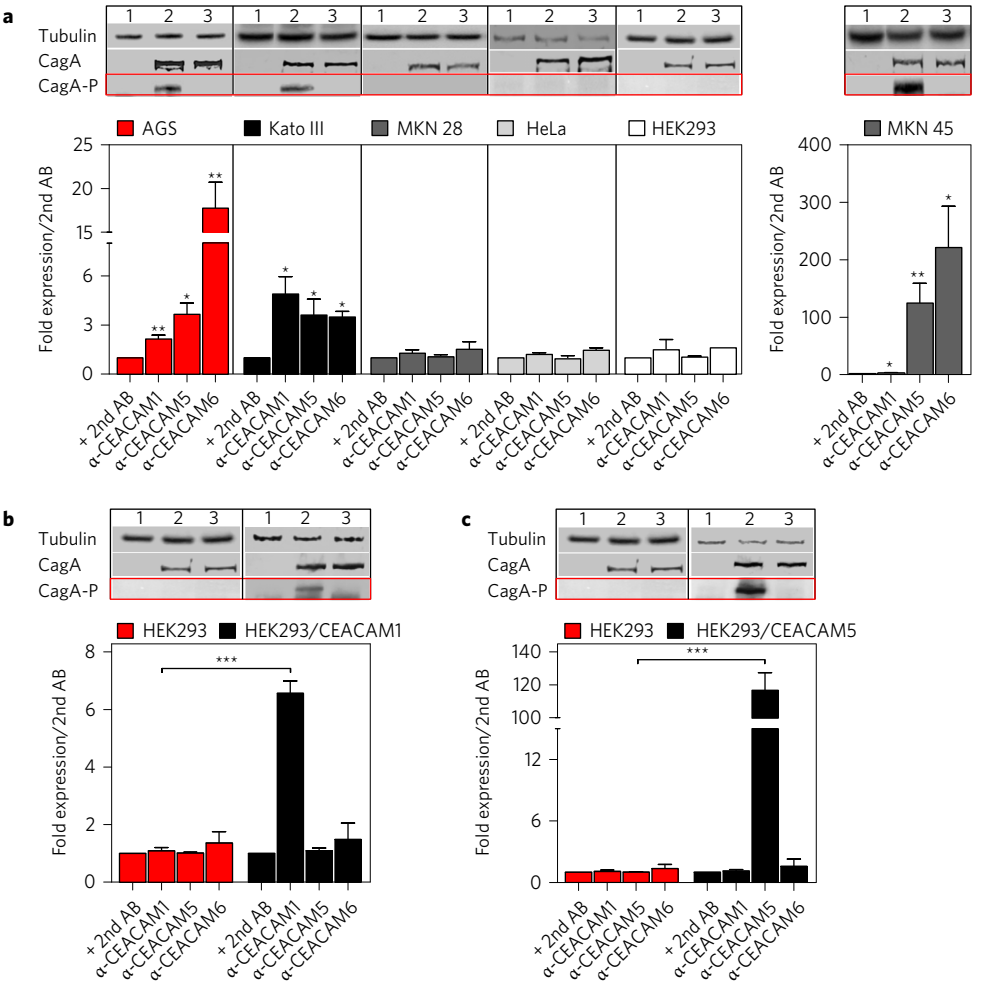

Figure 3 | The HopQ-CEACAM interaction is essential for *Hp* CagA translocation. a, Correlation between CEACAM1, CEACAM5 or CEACAM6 expression and CagA injection by *Hp*. Human gastric (AGS, Kato III, MKN28, MKN45) and non-gastric (HeLa, HEK293) cell lines produce CEACAM1, CEACAM5 or CEACAM6 on their surface, as measured by flow cytometry. *Hp* infection leads to translocation and phosphorylation of CagA (lane 1, non-infected cells; lane 2, *Hp* P12; lane 3, P12Δ*cagI*, red box). **b**,**c**, HEK293 cells were stably transfected with expression plasmids producing human CEACAM1 (**b**) or CEACAM5 (**c**) and cell surface localization of the proteins was determined by flow cytometry. Immunoblots demonstrate the capacity of *Hp* P12 to inject CagA into HEK293 (left blocks, red box) or HEK293/CEACAM1/CEACAM5 (right blocks, red box) cells. Student's *t*-test: two-tailed (**a**) and one-tailed (**b**,**c**); $^{*}P < 0.05$, $^{**}P < 0.01$, $^{***}P < 0.001$. Values are means ± s.e.m. Western blots show representative results of experiments that were performed three times.

e). In contrast, Kato III cell binding of the mutant strain did not show any significant differences from the WT strain, whereas the complemented strain showed enhanced binding (Supplementary Fig. 6c,f). Our data suggest that on AGS and Kato III cells additional receptors besides CEACAMs are present, whereas in MKN45 cells CEACAMs might represent the major receptor for *Hp*. Generally, HopQ seems to efficiently recruit and cluster CEACAM5 on the surface of the host cells and even cover *Hp* partially or completely. These data are corroborated by the CagA translocation results, showing a correlation between CEACAM adhesion capability of *Hp* and CagA translocation (Supplementary Fig. 5b–e), suggesting that adherence via outer membrane proteins is a prerequisite for CagA translocation by *Hp*.

Pathology and stabilization of the *cag*-T4SS in the CEACAM5-humanized mouse model. To further study the role of a putative HopQ-mediated adhesion in the stomach mucosa, we used the Mongolian gerbil and mouse models. The gerbil-adapted *Hp* strain P322 and an isogenic *hopQ* knockout strain revealed a similar colonization rate (Supplementary Fig. 7a), no significant differences in pathology scores[28] (Supplementary Fig. 7b) and a HopQ-independent binding to gerbil gastric tissue sections (Supplementary Fig. 7c–e). This suggests that no compatible CEACAM receptor(s) for HopQ-mediated binding of *Hp* is/are present on gerbil antrum or corpus tissue, although we cannot rule out a denaturation of CEACAM IgV protein domains in fixed gastric sections.

Because mice generally do not have a CEACAM5 gene[29] and murine CEACAM1 is not recognized by *Hp* (Supplementary Fig. 2a), a transgenic C57BL/6 mouse expressing the human CEACAM5 gene (CEACAM5-humanized mouse, here designated 'CEA mouse')[30] was used to further study *Hp* CEACAM interactions. The production of human CEACAM5 in the mouse gastric mucosa was verified by immunostaining (Supplementary Fig. 8a,b).

Infection experiments by the mouse-colonizing *Hp* strain PMSS1 revealed a similar rate of colonization for C57BL/6 WT and CEA mice after 6 weeks, 3 months or a long-term infection of 12 months (Supplementary Fig. 8c–e). The histopathological evaluation of mouse stomach tissue did not show significant differences in activity or chronicity of CEA- versus WT-infected animals up to 3 months of infection (Supplementary Fig. 9a), but the long-term infected animals showed a significant difference in the activity of gastritis after 12 months ($P < 0.05$) (Supplementary Fig. 9b). Re-isolated *Hp* from CEA versus WT mice after 6 weeks, but not after 3 months or 12 months of infection showed a significantly

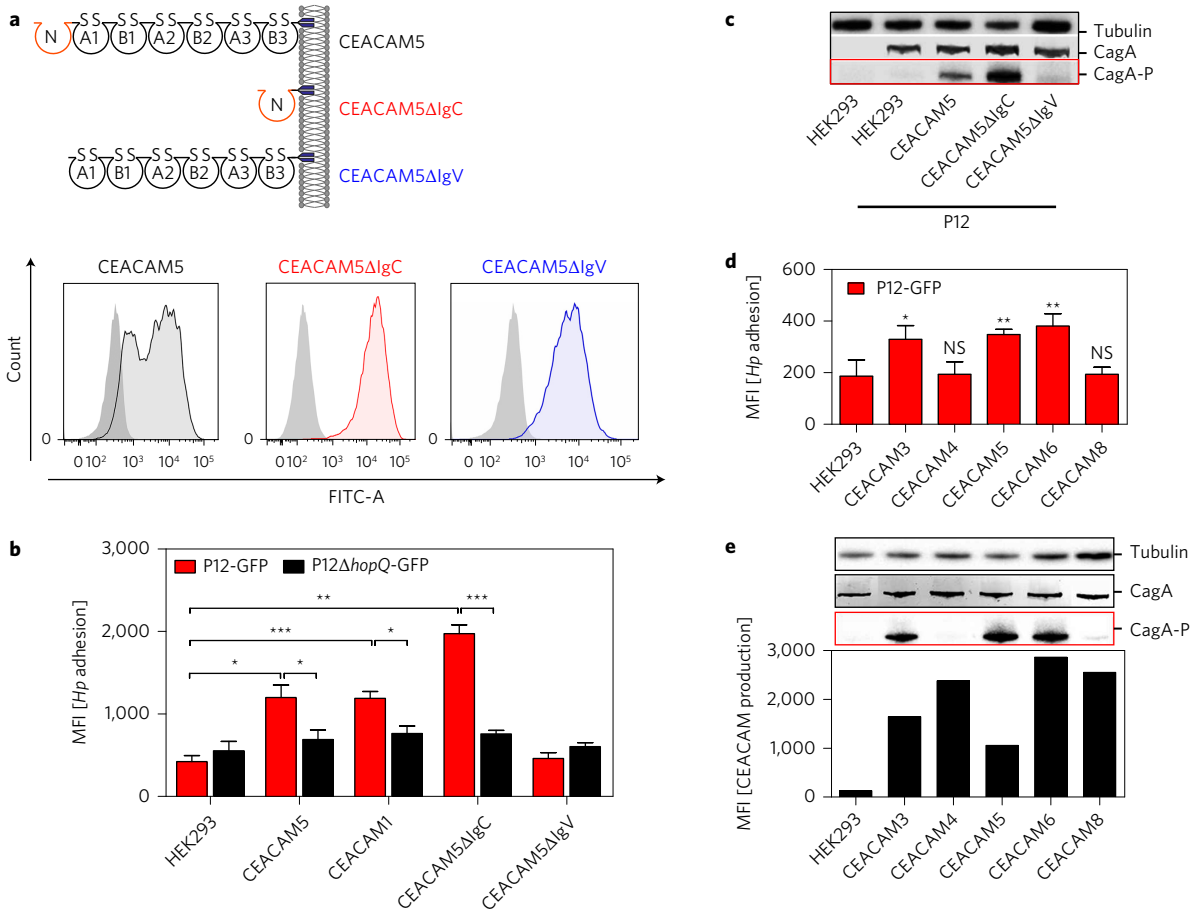

Figure 4 | CEACAM1, CEACAM3, CEACAM5 and CEACAM6 act as cellular receptors for *Hp*, and the N-terminal IgV domain of CEACAM5 is sufficient to mediate CagA translocation. a, Construction of expression plasmids producing truncated versions of CEA containing the N-terminal IgV domain (CEACAM5ΔIgC) or the constant domains only (CEACAM5ΔIgV). Transfection into HEK293 cells resulted in stable cell lines producing the variant forms on their surface, as determined by flow cytometry using anti-Pan-CEACAM (for CEACAM5ΔIgC) or anti-CEACAM5 (for CEACAM5 or CEACAM5ΔIgV) antibody. **b**, Bacterial binding of *Hp* P12 or P12Δ*hopQ* to HEK293 or stable CEACAM1- or CEACAM5-transfected HEK293 cells, CEACAM5ΔIgC or CEACAM5ΔIgV, as determined by flow cytometry of GFP-labelled *Hp* strains. **c**, Infection of HEK293 cells, or HEK293 cells stably producing CEACAM5, CEACAM5ΔIgC or CEACAM5ΔIgV, with *Hp* P12. CagA translocation (CagA-P) is shown by western blot using the phosphotyrosine-specific antibody 4G10. **d**, Bacterial binding of *Hp* P12 to HEK293 or transiently transfected HEK293 cells. **e**, Bottom: transient transfection of HEK293 cells with CEACAM plasmids (Supplementary Table 4) and determination of relative surface localization of the proteins (MFI) by flow cytometry using specific antibodies (one representative experiment is shown). Top: immunoblot showing CagA injection (CagA-P) of *Hp* P12 into transiently transfected CEACAM-expressing HEK293 cells (red box). Statistics: *t*-test, one-tailed (comparison of HEK293 and CEACAM-transfected cells) (**d**) and one-way ANOVA with Dunnett's multiple comparisons test as post hoc analysis, one-tailed (**b**); $*P < 0.05$, $**P < 0.01$, $***P < 0.001$. Values (**b**,**d**) are means ± s.e.m. Experiments show representative results and were performed three times.

higher rate of bacteria with a functional *cag*-T4SS, as measured by their capability for CagA translocation into AGS cells (Supplementary Fig. 9c). After 3 and 12 months of infection, the capacity for IL-8 induction by *Hp* was significantly reduced in CEA as compared to WT-infecting re-isolates (Supplementary Fig. 9f–h).

Collectively, these data suggest that in the early phase of infection (6 weeks) a stronger adhesion of *Hp* in the CEA as compared to the WT mouse gastric mucosa might increase gastric inflammation and the host immune response. Subsequently, according to the rheostat model[31], the stimulated inflammation would provoke *Hp* in CEA mice to more quickly switch off the *cag*-T4SS to avoid its elimination, supporting a role for CEACAM5 as a functional receptor in this mouse model *in vivo*.

Expression of CEACAM5 in the infected human stomach is *cag*-T4SS-dependent. To further evaluate the role of CEACAMs during *Hp* infection in the human stomach, we characterized gastric biopsy isolates from *Hp*-infected patients for virulence traits (for example, functional *cag*-T4SS, CagA tyrosine phosphorylation in AGS cells, IL-8 induction). We therefore generated thin sections from formalin-fixed paraffin blocks for microscopy studies to determine the pathology, and classified the gastric biopsy material into three groups: (1) non-*Hp*-infected (by urea breath test (UBT) and culture, six biopsies), (2) infected with CagA-positive and translocation-competent *Hp* (CagA+P$^+$; 11 biopsies) and (3) infected with CagA translocation-negative (CagA+P$^-$) or CagA-negative (CagA−P$^-$) strains (four biopsies). Strikingly, CEACAM5 expression was significantly higher in CagA+P$^+$ strain infections relative to all others (Figs 5 and 6a). Despite a strong surface localization of CEACAM5 in CagA+P$^+$ infected patients, an AGS luciferase reporter cell line did not sense a direct transcriptional upregulation of CEACAM5 promoter-driven luciferase expression by the *Hp cag*-T4SS, or phosphorylated injected CagA under *in vitro* infection conditions for up to 3 h (Supplementary Fig. 10). These data suggest that not *Hp* per se, but the inflammation, or the specific cytokine milieu induced by CagA+P$^+$ *Hp* infection in the

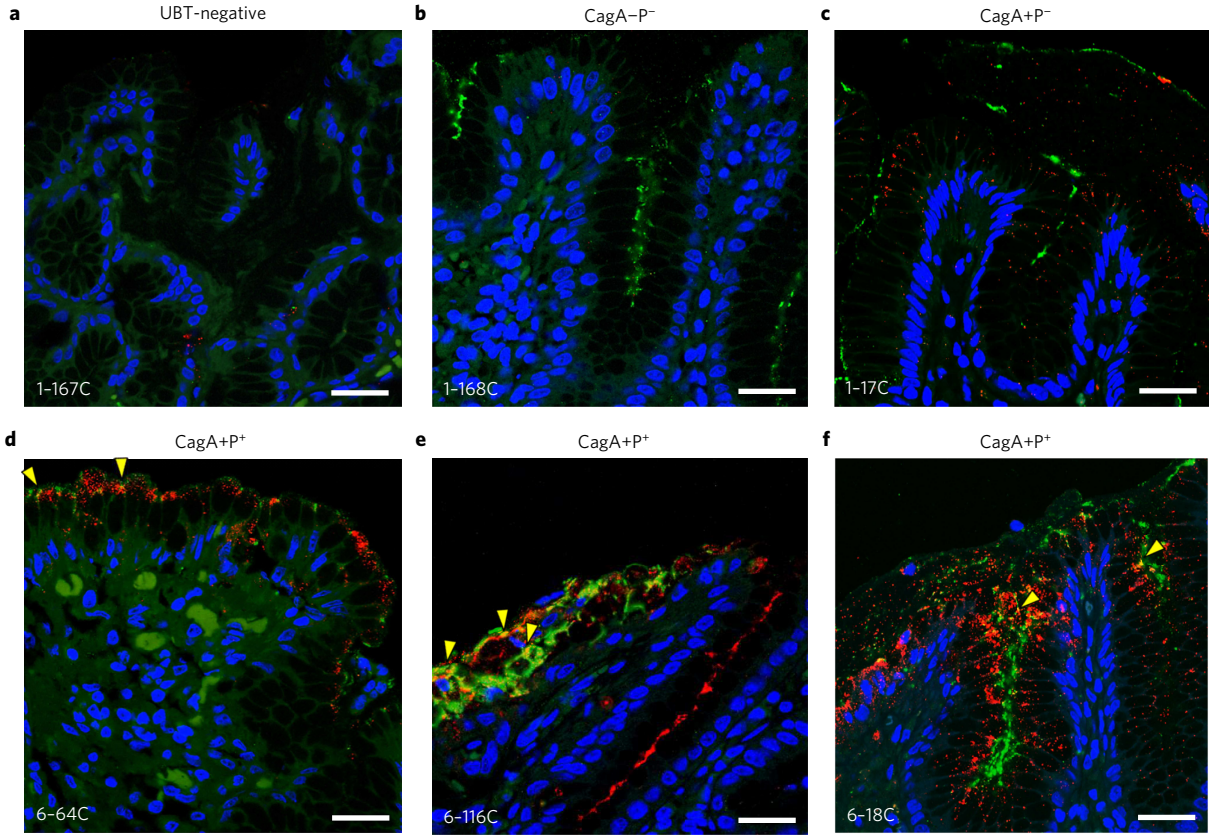

Figure 5 | *Hp* co-localizes with CEACAM5 in the gastric tissue of *Hp*-infected patients. a–f, Thin sections (10 μm) of paraffin-fixed corpus biopsy material from an *Hp*-negative patient (patient 1-167C) (**a**) or *Hp*-positive patients infected with a CagA−P$^-$ strain (patient 1-168C) (**b**) or a CagA + P$^-$ strain (patient 1-17C) (**c**) or with different CagA+P$^+$ strains (patients 6-64C, 6-116C and 6-18C) (**d–f**). Sections were stained with DAPI (blue), with α-*Hp* antibody (green) and with α-CEACAM5 antibody (red) and visualized by a Leica SP5 confocal microscope. Bacteria are located on top of epithelial cells (green), CEACAM5 staining is mainly on the apical side of the epithelial cells. Co-localization of *Hp* and CEACAM5 (yellow) indicates co-localization (yellow arrowheads). Scale bars, 50 μm. At least three independent micrographs of each biopsy section were taken and one representative area is shown.

gastric mucosa, might be driving CEACAM5 expression in infected tissue.

Discussion

We have discovered here, for the first time, distinct members of the CEACAM protein family as novel protein receptors for *Hp*. In addition, the outer membrane protein HopQ, a member of the comprehensive *Hp* Hop protein family, could unambiguously be identified as a novel bacterial adhesin binding CEACAM receptors. We show that the IgV-like N-terminal domains of CEACAM1, CEACAM3, CEACAM5 and CEACAM6 are sufficient for *Hp* binding. The HopQ–CEACAM binding is essential for CagA injection into host cells carrying no additional receptors for *Hp* binding (for example, HEK293 cells transfected with human CEACAMs, MKN45 cells). Thus, CagA injection correlates with the binding capacity of *Hp* to the corresponding host cells. These results also indicate that a direct binding of components of the *cag*-T4SS (CagL, CagA, CagY and CagI) to β_1 integrin receptors[3,4] is not sufficient for CagA translocation by *Hp*. Instead, apart from integrin binding, interaction of at least one outer membrane adhesin with a distinct cellular receptor (for example, HopQ–CEACAM, or another adhesin-receptor pair) is required.

Binding experiments with soluble CEACAM IgV constructs, or recombinant HopQ and CEACAM domains in ITC experiments, showed that binding of *Hp* is highly specific, strong and independent of glycosylation of CEACAMs. HopQ does not recognize murine, canine or bovine CEACAM receptors, which clearly underpins the very high species adaptation during a long co-evolution of *Hp* with humans[32]. We also did not detect a specific binding of the HopQ adhesin to the antrum or corpus of Mongolian gerbil tissue, suggesting that no compatible CEACAM receptor(s) for HopQ-mediated binding of *Hp* is/are present on gerbil antrum or corpus tissue. In the humanized CEACAM5 mouse, we observed a CEACAM5-dependent effect concerning gastritis activity after 12 months of infection, indicating that CEACAM receptors play a role for *Hp* infection and might have long-term consequences *in vivo*, but further work will be necessary to determine the role and functional consequences of the HopQ–CEACAM interaction *in vivo*.

In gastric sections of *Hp*-infected patients we observed a significantly higher CEACAM5 expression in the corpus versus the antrum of the patient gastric mucosa (Fig. 6a), suggesting that CagA+P$^+$ *Hp* strains might exploit the inflammatory conditions to more efficiently adhere to the gastric corpus. Although our *in vitro* CagA translocation data show a correlation between the amount of CEACAM expressed on the cell surface and CagA translocation efficiency (Fig. 3), it remains at present unclear whether upregulated CEACAM5 expression in the gastric corpus enhances CagA delivery *in vivo*. CagA-P$^-$ or CagA + P$^-$ *Hp* are seen on the surface of gastric sections (Fig. 5b,c). However, these bacteria do not co-localize with CEACAM5 (Fig. 5b,c), which is in contrast to the CagA+P$^+$ *Hp* strains, which often show intimate contact with CEACAM5, suggesting direct adhesion. Thus, our data support the general finding that CagA+P$^-$ and CagA−P$^-$ *Hp* strains are mainly located in the mucus layer, or adherent to surface-associated glycoprotein receptors, such as Lewis^b or other Lewis antigens, rather than on the epithelial cell surface or in the tissue.

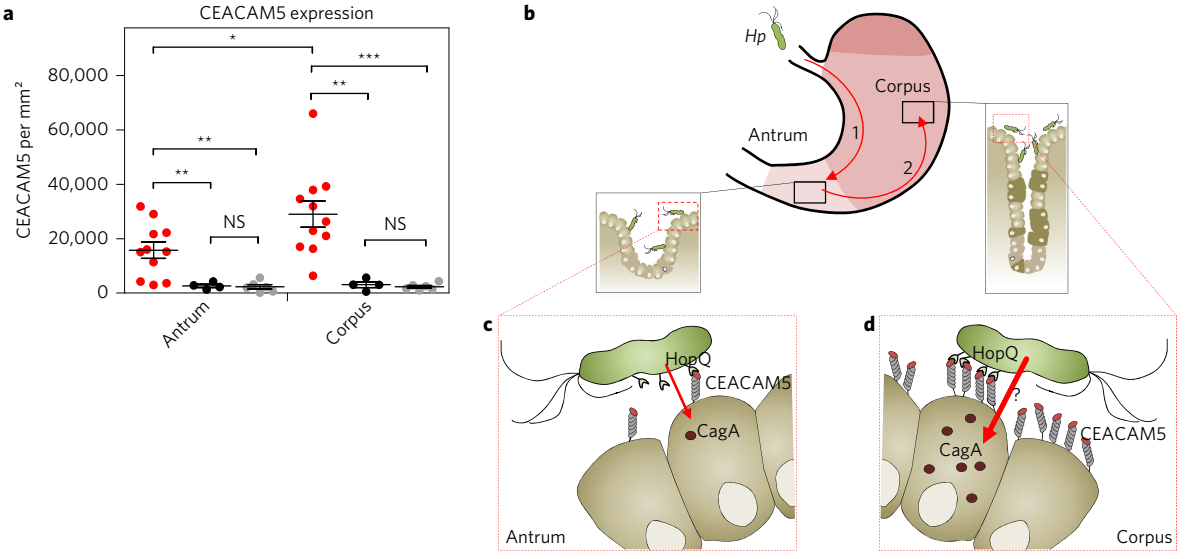

Figure 6 | CEACAM5 expression levels determined on human gastric biopsy sections. a, Gastric paraffin sections of the antrum and corpus region of 11 patients infected with CagA+P$^+$ strains (red circles), four patients infected with CagA–P$^-$ strains (blue circles) and five non-infected patients (grey circles) were analysed for CEACAM5 expression levels (CEACAM5 per nm^2). **b**–**d**, Model of *Hp* colonization of the human gastric mucosa showing HopQ-mediated binding of CEACAM5 in the antrum (**b**,**c**). After the initial infection of the antrum of the human stomach (1), *Hp* usually stably colonizes. *Hp* binds via its outer membrane adhesin HopQ to the N-terminal IgV-like domain of CEACAM5, which enables CagA+P$^+$ bacteria to inject their effector protein CagA. *Hp* might spread from the antrum to the corpus region (**d**) (2) (pangastritis) and might bind to epithelial cells with high CEACAM5 production, possibly supporting an enhanced CagA translocation (red arrow). Statistics: Mann–Whitney *U*-test two-tailed; $*P < 0.05$, $**P < 0.01$, $***P < 0.001$. Values are means ± s.e.m., $n = 11$ for CagA+P$^+$, $n = 4$ for CagA+P$^-$/CagA–P$^-$ strains.

Hp might also encounter other human CEACAMs in the gastric mucosa, such as CEACAM1, or the granulocyte-specific member of the CEACAM family, CEACAM3, which was identified as the major receptor responsible for opsonin-independent phagocytosis and bacterial elimination[33]. By contacting these receptors, *Hp* might induce intracellular signalling events via stimulation of immunoreceptor tyrosine-based inhibition motifs (ITIM) or immunoreceptor tyrosine-based activation motifs (ITAM) in the cytoplasmic tail of CEACAM1 or CEACAM3, respectively. A better understanding of the molecular details of these interactions could help to understand the strategies of *Hp* for chronic infection and consequently to devise better treatment schemes against *Hp* infections.

Methods

Bacterial strains and cell culture. *Hp* strains were cultured at 37 °C under microaerophilic conditions on GC agar plates (Oxoid) supplemented with vitamin mix (1%), horse serum (8%), trimethoprim (5 μg ml^{-1}) and nystatin (1 μg ml^{-1}) (serum plates). Chloramphenicol (6 μg ml^{-1}), kanamycin (8 μg ml^{-1}) or streptomycin (250 μg ml^{-1}) were added to select for transformants or screen colonies for resistance to either drug, when necessary. Plates were incubated for 24–48 h under microaerobic conditions (85% N_2, 10% CO_2, 5% O_2) at 37 °C. *Moraxella catarrhalis* strains 11994 and 9143 were incubated at 37 °C using Columbia blood agar plates (Oxoid). The gerbil-colonizing strain P322 (*cag*-PAI positive, vacAs1m1, *hopQ* I), a patient isolate, was passaged several times through the gerbil stomach. All bacteria were passaged two to three times before the first experiments were performed. The agar plates contained GC (Oxoid) supplemented with 8% horse serum (PAA) and 1% vitamin mix (100 g l^{-1} D-glucose, 10 g l^{-1}L-glutamine, 26 g l^{-1}L-cystein, 0.1 g l^{-1} co-carboxylase, 20 g l^{-1} Fe(III) nitrate, 3 g l^{-1} thiamin, 13 mg l^{-1} *p*-aminobenzoic acid, 250 mg l^{-1} nicotinamide-adenine dinucleotide, 10 mg l^{-1} guanine, 0.15 g l^{-1} L-arginine and 0.5% uracil). All cells were grown at 37 °C and 5% CO_2 and subcultured every 3–4 days. AGS and HeLa cells were grown in RPMI/10% FCS, MKN45 cells in RPMI/20% FCS and Kato III cells in DMEM/20% FCS. For MKN28, RPMI medium was supplemented with 10% FCS, 10 mM HEPES, 1 mM sodium pyruvate and 0.1 mM non-essential amino acids. HEK293 cells were cultured in DMEM/15% FCS and supplemented with 1 mg ml^{-1} G418 when they were transfected with CEACAM constructs. All cell lines used in this study are routinely tested for mycoplasma contamination (once a year) and proved to be negative (4′,6-diamidino-2-phenylindole (DAPI) staining; LookOut Mycoplasma PCR Detection Kit, Sigma Aldrich, catalogue no. MP0035). Cells are routinely checked for their morphology (size, granularity), growth behaviour and species identity (human cell lines). All cell lines used have been verified by a cell line authentication test (Eurofins Medigenomics). AGS cells (CRL-1739) and Kato III cells (HTB-103) were purchased from ATCC, HEK293 cells from Tularik (taken over by Amgen) and MKN45 cells (ACC 409) from DSMZ.

Plasmids for bacteria and eukaryotic cell manipulation. *Hp* strain P12 was used for the generation of marker-free outer membrane protein mutants. OMP genes *babA*, *babB*, *sabB*, *hopZ* and *hopQ* were deleted using the contra-selectable streptomycin susceptibility method, as described in ref. 34. The up- and downstream regions of the gene of interest were cloned in a pBluescript II SK(+) vector (Agilent Technologies) flanking a resistance cassette. Primers used for amplification of DNA fragments adjacent to the genes encoding outer membrane proteins are listed in Supplementary Table 2. In strain P12, two identical gene copies of *babB* (in the *babB* and *babC* loci) and *sabB* (in the *sabB* and *sabA* loci) had to be deleted to obtain marker-free mutants. By homologous recombination of the adjacent gene regions, the resistance marker was first inserted in the locus of the gene of interest, creating the distinct outer membrane protein gene mutant strain. In the second step, the resistance cassette was completely removed, resulting in a marker-free mutant strain according to the contraselection method[34]. P12Δ*cagI* was generated using the method described above and served as negative control for CagA translocation competence in all *in vitro* infection experiments[35]. For genetic complementation of the *hopQ* mutant, the P12 gene was cloned in an *E. coli–H. pylori* shuttle vector based on the pHel3 plasmid of *Hp*, as described in ref. 18.

Mammalian expression plasmids encoding the GFP-tagged amino-terminal IgV-like domains of human CEACAM1 (hCEA1-N), murine CEACAM1 (mCEA1-N), bovine CEACAM1 isoforms a or b (bCEA1a-N or bCEA1b-N, respectively), as well as canine CEACAM1 (cCEA1-N) have been described previously[36]. The CEACAM5 orthologue from *Macaca mulatta* was constructed by using macaque cDNA (reverse transcribed from mRNA derived from a colon tissue biopsy and generously provided by C. Roos, German Primate Center, Göttingen, Germany) and amplifying the coding sequence for the amino-terminal IgV-like domain of macaque CEACAM5 with primers macCEA-IF-sense′ and CEACAM5-NT-IF-anti (Supplementary Table 2). The resulting PCR fragment was cloned into pDNR-Dual using the In-Fusion PCR Cloning Kit (Clontech) and transferred by Cre-mediated recombination into pLPS-3′ EGFP (Clontech) resulting in GFP fused to the carboxy-terminus of the expressed protein.

For the cloning of HopQ and CEACAM N-terminal domains, HopQ (residues 25–460, *Hp* strain P12) was cloned into a *NotI/XhoI* modified pET21d vector containing an N-terminal maltose binding protein-tag (MBP, containing several mutations: D82A/K83A/E172A/N173A/K239A) and a C-terminal hexa-histidine tag. Human CEACAM5 (residues 34–141, CEA-N) was cloned into a *NcoI/XhoI* cut pET21d vector with a stop codon before the hexa-histidine tag. CEACAM1, CEACAM3 and CEACAM8 were synthesized and codon optimized as GeneArt Strings (Life Technologies). GeneArt Strings were cut and cloned into an NcoI/XhoI cut pET21d vector without a purification tag.

Mammalian expression plasmid pRc/CMV-CEA has been described previously[37]. CEACAM5 truncations were constructed by PCR using inverted phosphorylated primers and subsequent *DpnI* digestion followed by ligation. Deletion of IgC-like domains was performed with primers LH90/LH91, resulting in plasmid pLH45 and deletion of IgV-like domains with primers LH79/LH89 (Supplementary Table 2) leading to pLH46.

Bacterial pulldown assay. The bacterial pulldown was performed as described in ref. 24. Bacteria of an overnight culture were resuspended in 1 ml PBS and the optical density at 550 nm (OD_{550}) was measured. A total of 4×10^6 bacteria, calculated by the OD_{500} measurement, were incubated with cell culture supernatants containing CEA-N-GFP. After an incubation time of 30 min at room temperature with head-over-head rotation, the bacteria were washed twice with PBS containing 0.9 mM $CaCl_2$ and 0.5 mM $MgCl_2$ and resuspended in SDS loading buffer. After heat denaturation, the samples were analysed by western blotting as described previously[24]. Alternatively, bacteria were resuspended in PBS/2% FCS and analysed by flow cytometry (FACS Canto II, BD Biosciences).

Protein expression of MBP–HopQ and MBP–CEACAM5 in *E. coli* and purification. HopQ, MBP and CEA-N were expressed in *E. coli* BL21(DE3) pLysS cells. Cells were grown at 37 °C until an absorbance at 600 nm (A_{600}) of 0.6 and were induced with 1 mM isopropyl-β-D-thiogalactopyranoside and grown for 4 h at 37 °C (CEACAMs) or 18 °C (HopQ or MBP). HopQ and MBP cells were resuspended in ice-cold 20 mM Tris, 500 mM NaCl, pH 7.5 (NiBB) and lysed by sonication. HopQ and MBP were purified by nickel affinity chromatography (HisPur Ni-NTA Resin, Thermo Scientific) by passing the soluble fraction over the beads and removing unbound protein with 20 ml of NiBB. Beads were further washed with NiBB, 50 mM imidazole, pH 7.5 (15 ml) before elution with NiBB, 400 nM imidazole, pH 7.5 (10 ml). The elution and wash steps were combined and diluted twofold with 20 mM Tris, 150 mM NaCl, 1 mM EDTA, pH 7.5 (amylose binding buffer) and loaded onto amylose resin (NEB). Resin was washed with 30 ml of amylose binding buffer and protein eluted with 15 ml of amylose binding buffer containing 40 mM maltose. HopQ and MBP were further purified by size exclusion chromatography using a Superdex 200 column (GE Healthcare) equilibrated with 20 mM Tris, 150 mM NaCl, 40 mM maltose, pH 7.5. CEACAM cells were resuspended in ice-cold NiBB, 10 mM EDTA, 1% vol/vol Trition-X-100 and lysed by sonication. The soluble fraction was discarded and inclusion bodies resuspended in the same buffer and further disrupted by sonication. Inclusion bodies were then washed with 50 mM Tris, 1 M NaCl, pH 8.0 and then NiBB. Inclusion bodies were finally dissolved in 30 mM Tris, 150 mM NaCl, 8 M urea, pH 8.3 and CEACAMs refolded at 4 °C by diluting the redissolved inclusion bodies slowly (100 µl min^{-1}) 1:20-fold into 50 mM *N*-cyclohexyl-2-aminoethanesulfonic acid (CHES), 500 mM L-arginine, pH 9.2, overnight. Refolded CEACAMs were dialysed against 50 mM Tris, pH 8.0 and concentrated by MonoQ (GE Healthcare). CEACAMs were further purified by size exclusion chromatography using a Superdex 200 column equilibrated with 30 mM Tris, 150 mM NaCl, pH 8.3. See Supplementary Table 2 for oligonucleotides and Supplementary Table 4 for plasmid constructs.

Isothermal titration calorimetry (ITC). All proteins were dialysed against 30 mM Tris, 150 mM NaCl, 5 mM maltose, pH 7.5. ITC experiments were performed using an iTC200 instrument (GE Healthcare). A typical experiment consisted of loading the syringe with CEACAM (240 µM) and MBP or HopQ placed in the cell (24 µM). Titrations were performed at 25 °C with 17 injections of 2.46 µl aliquots, with 210–240 s intervals between injections. For CEACAM8, the number of injections was decreased but larger volumes were injected. Heats of dilutions were also measured and subtracted from each data set. CEACAM5 binding to MBP alone was also tested. All data were analysed using Origin 7.0 software.

Infection experiments of eukaryotic cell lines. Before infections, cells were overnight serum-starved using cell culture medium without FCS. The next morning, cells were grown for 2 h in PBS containing 10% FCS and then infected with bacteria. In all experiments, a MOI (multiplicity of infection) of 60 was used and the infection was stopped after 4 h on ice. Cells were collected in PBS containing 1 mM sodium vanadate, 1 µM leupeptin, 1 µM pepstatin and 1 mM phenylmethylsulfonyl fluoride and resuspended in SDS loading buffer. Equal amounts of samples were loaded on a gel and analysed by western blotting.

Antibodies used for flow cytometry or western blotting. For the detection of CEACAM-N-GFP constructs in the bacterial pulldown, monoclonal GFP antibody (clone JL-8, Clontech) was used. The densitometry of GFP signals was evaluated by Image Lab 4.1 software, and the band intensity was normalized against rabbit polyclonal AK263 (α-RecA) antibody signals[38]. In the *in vitro* infection model, polyclonal rabbit anti-CagA antibody (AK257)[5] was used to detect CagA, monoclonal anti-phosphotyrosine antibody (clone 4G10, Millipore) was used to monitor CagA tyrosine phosphorylation, AK268 (ref. 39) for the detection of CagA, and anti-tubulin antibody (Abcam) for normalization of cell lysates.

The antibody AK298 (this study) was generated against a conserved peptide sequence of HopQ (type I) of *Hp* strain P12 (SKGEKLEAHVTTSKYQ) by immunization of rabbits (Genosphere Biotech). The anti-peptide antibody was verified to be specific for HopQ type I by using a P12Δ*hopQ* strain and was used for the detection of HopQ.

Cells were stained with specific antibodies (Aldevron) against human CEACAM1 (clone GM-8G5), CEACAM5 (clone 6/3/13), CEACAM6 (clone 9A6), CEACAM8 (clone LT-3AG-B2) or pan CEACAM (clone D14HD11) according to the manufacturer's instructions and analysed in a flow cytometer (FACS Canto II, BD Biosciences).

HEK293 adherence assay. Cells were infected with GFP expressing *Hp* using an MOI of 60 for 1 h at 37 °C and 5% CO_2. After three washing steps with PBS containing 2% FCS, the cells were collected and analysed in a flow cytometer (FACS CantoII, BD Biosciences). The mean fluorescence intensity from non-infected cells was subtracted from infected samples. At least three experiments were performed and analysed with Student's *t*-test.

Transfection of HEK293 cells. HEK293 cells were transfected in 10 cm^2 culture dishes with Lipofectamine 2000 (Life Technologies) reagent following the manufacturer's recommendations. After 24 h, the cells were washed and 1 mg ml^{-1} geneticin (Life Technologies) was added to select for stably transfected cells. After 3–4 weeks of subculturing, cells were stained with monoclonal CEACAM antibodies (pan CEACAM clone D14HD11 or CEACAM5 clone 26/3/13, Aldevron, 1.2 µg per 10^6 cells) and subsequently with secondary Alexa488-coupled anti-mouse IgG antibody before FACS (FACS Aria-II, BD Biosciences). After sorting, the cells were reanalysed for CEACAM expression with a Canto-II (BD Biosciences) flow cytometer. The same protocol was used for transient transfections. Expression analysis was performed 24 h after transfection.

HEK293 cells were found to produce no CEACAM1, 5 and 6 on their surface. Furthermore, they are easily and efficiently transfected and proved to be free of mycoplasma. We therefore chose these cells for the stable CEACAM transfection experiments. In the International Cell Line Authentication Committee (ICLAC) database they are described as cross-contaminated with HeLa cells. Because we also tested HeLa cells as negative for CEACAM production, this cross-contamination did not interfere with the results of our experiments (for example, CagA translocation). MKN28 cells are also listed in the ICLAC database as cross-contaminated with human gastric MKN74 cells. MKN28 cells were identified as CEACAM-deficient and for this work only used to support the correlation between CEACAM surface expression and CagA translocation capability of *Hp*.

CEACAM5-luciferase reporter assay. For construction of the CEACAM5 promoter plasmids pGL4.21-CEACAM5_P0.4Kb and pGL4.21-CEACAM5_P3.1Kb, a 430 bp or a 3,109 bp region upstream of the CEACAM5 gene was amplified by PCR using a plasmid template pCEA3300 with primers ZQ113 and ZQ112 or ZQ111 and ZQ112, respectively, and cloned into the EcoRV and HindIII sites of pGL4.21 (Promega). AGS cells were co-transfected with pGL4.21-CEACAM5 promoter plasmids and the internal control pGL 4.74 (Promega) in the ratio 1:1, except the promoter-less control comprised AGS cells co-transfected with empty vector pGL4.21 and the internal control pGL4.74 ($n = 3$). Transiently transfected AGS cells were infected with *H. pylori* strains at an MOI of 60 for 3 h at 37 °C, 5% CO_2. Firefly luciferase and Renilla luciferase activities were measured with a Dual-Glo Luciferase Assay system (Promega). Transfection control was normalized as 1.

CEACAM knockdown in AGS cells. AGS cells were transfected with Hs_CEACAM1_11 siRNA (CTGCACAGTACTCCTGGCTTA) targeting CEACAM1, CEACAM5 and CEACAM6, Hs_CEACAM5_6 (CGCAGTATTCTTGGCGTATCA), Hs_CEACAM6_7 (AAGAAG ATAGATCCAATTAAA) (Qiagen) and AllStars Negative Control siRNA (Qiagen) by Lipofectamine RNAiMAX (Invitrogen) according to the manufacturer's instructions. After 48 h, the siRNA effect on expression of CEACAM1, 5 and 6 was evaluated against AGS control cells by flow cytometry analysis (FACS Canto II, BD Biosciences). AGS control cells and AGS/CEACAM-siRNA with a downregulation of CEACAM1, CEACAM5 and CEACAM6 were infected with *Hp* strains and tested for CagA translocation.

Immunofluorescence of gastric epithelial cell lines AGS, Kato III and MKN45. AGS and Kato III cell lines were cultured in RPMI medium supplemented with 10% fetal calf serum (Gibco–Life Technologies). For cell line MKN45, RPMI medium supplemented with 20% fetal calf serum (Gibco–Life Technologies) was used. All cell lines were cultured at 37 °C and 5% CO_2. For immunofluorescence, cells were seeded on sterile cover slides in a 24-well plate (Costar) at a cell density of 2×10^5 cells per cm^2 and cultivated further. After 2 days, cells were infected with *Hp* WT or isogenic mutant strains with an MOI of 10 for 4 h at 37 °C and 5% CO_2. For immunostaining, cells were fixed with 4% paraformaldehyde for 10 min and subsequently blocked with 2% fetal calf serum in PBS (Gibco–Life Technologies) overnight. Fixed cells were incubated with mouse anti-CEACAM5 (1:300, clone 26/3/13, Aldevron) and rabbit anti-*Hp* (1:400, AK175) for 1 h at room temperature. After washing with DPBS, cells were incubated with secondary antibodies (1:1,000, goat anti-rabbit Alexa Fluor 488, goat anti-mouse Alexa Fluor 555; Invitrogen - ThermoFischer Scientific) and Alexa Fluor 647 phalloidin (300 U) (1:1,000; Invitrogen–ThermoFischer Scientific) for 1 h at room temperature in the dark. Afterwards, cell nuclei were stained with DAPI (5 µg ml^{-1}; Sigma) for 5 min. Samples were mounted with Mowiol (Sigma). Pictures were taken with a CLSM

(Leica SP5) with a ×63 oil immersion objective (HCX PL APO lamda blue ×63, 1.4 oil). Image processing was performed with LAS AF software (Leica).

Mouse and Mongolian gerbil infections

Mice. Specific-pathogen-free, transgenic C57BL/6_CEACAM5± mice (*Mus musculus*) were bred, infected and killed at the Max von Pettenkofer-Institut (Munich, Germany). The animals (males and females) were infected orogastrically three times on three subsequent days with a dose of 10^9 bacteria. Animals were infected with *Hp* strain PMSS1 at between 8 and 12 weeks of age. Littermates not expressing the CEA5 receptor (C57BL/6_CEACAM5−/−, here designated WT) were inoculated with identical volumes and preparation of bacteria. All experiments and procedures were conducted in accordance with the guidelines for the care and use of laboratory animals and approved by the Regierung von Oberbayern (AZ 55.2-1-54-2532-34-14). Groups of animals ($n = 10$) were killed after 6 weeks, 3 or 12 months.

Mongolian gerbils. Specific-pathogen-free Mongolian gerbils (*Meriones unguiculatus*, outbred) were bred, infected and killed at the Max von Pettenkofer-Institut. The animals (males and females) were infected orogastrically three times on three subsequent days with a dose of 10^9 bacteria. Animals were infected with the *Hp* strain P322wt ($n = 10$) and P322wtΔ*hopQ* ($n = 11$) at between 8 and 14 weeks of age. All experiments and procedures were conducted in accordance with the guidelines for the care and use of laboratory animals and approved by the Regierung von Oberbayern (AZ-55.2-1-54-2532-1-11). Animals were killed after 8 weeks.

Sample-taking from animals. Animals were killed with CO_2. Blood was taken via cardiocentesis and serum was obtained by centrifugation. Stomachs were opened along the greater curvature and washed with PBS. The whole stomach was divided into two equal halves. One half was homogenized (glass homogenizer, Ochs) in brucella broth (BB) medium for isolation of bacteria. For mice, the other half was fixed in Tissue-Tek O.C.T Compound (Sakura) and for Mongolian gerbils the other half was fixed in formalin for immunohistology. Appropriate dilutions of homogenates were spread on selective serum plates (GC agar Difco). The number of colony forming units (c.f.u.) was calculated per gram of gastric tissue.

Immunohistology. Mouse stomachs were opened along the lesser curvature, flushed with ice-cold PBS and fixed in PBS-buffered 4% formaldehyde at room temperature (2 h) for paraffin-embedded tissues. Serial 3 µm paraffin sections were dewaxed and subjected to heat antigen retrieval at pH 9.0 (Target Retrieval Solution; Dako). After blockage of endogenous peroxidase, tissue sections were incubated with primary antibodies (α-CEACAM5, Dako, A011502, 1:350) for 1 h at room temperature or overnight at 4 °C, then with horse radish peroxidase-coupled secondary antibodies and 3-amino-9-ethylcarbazole (ImmPRESS Anti-Rabbit Ig Polymer Detection Kit; Vector Labs) and counterstained with haematoxylin.

Grading of inflammation. H&E-stained longitudinal paraffin sections of antrum and corpus were graded on the intensity of inflammation, metaplasia and ulcer development (scale 0–5) by a pathologist blinded to the treatment, according to Garhart and co-authors[28].

Immunofluorescence of gastric biopsies. Paraffin sections of antrum and corpus were deparaffinized and treated with citrate buffer for antigen retrieval (microwave). Sections were blocked with 5% goat serum in PBS and incubated with mouse anti-CEACAM5 (Aldevron) and rabbit anti-*Hp* (AK175), or mouse anti-CagA (Antibodies Online). After washing, the secondary antibodies were applied (goat anti-rabbit Alexa488 and goat anti-mouse Alexa555; Invitrogen) and incubated. Cell nuclei were stained with DAPI. Micrographs were taken with an epifluorescence microscope (Olympus BX61) ×40 objective and a CLSM (Leica SP5) with a ×63 oil immersion objective.

Data analysis. Measurements were performed with Volocity (Perkin Elmer) using the images taken from the CLSM Leica SP5. Briefly, CEACAM5 expression was evaluated as follows. Gastric sections were screened for the highest expression of CEACAM5 and the area of the CEACAM5 signal was then normalized to the whole epithelial cell area (CEACAM5 per nm^2) (Fig. 6a).

Tetramethyl-rhodamine (TAMRA) labelling of Hp and ex vivo gastric tissue infections. Labelling and infection was performed as described earlier[40]. In brief, a suspension of *Hp* in PBS (500 µl, $OD_{550} = 1.0$) was mixed with 2 µl TAMRA (5-(and 6)-carboxytetramethylrhodamine succinimidyl ester, mixed isomers, Molecular Probes; 10 mg ml^{-1} in DMSO) and incubated in the dark for 30 min. Bacteria were then washed three times with PBS/0.05% Tween20/1% bovine serum albumin (BSA) and resuspended in 500 µl PBS for direct use. Biopsy sections (cryo-sections) were cut and fixed on microscope slides with ice-cold acetone, rehydrated in PBS (10 min, 4 °C) and blocked with BSA (1%, 1 h, 37 °C). TAMRA-labelled *Hp* was added and incubated for 1 h at 37 °C and 5% CO_2. To remove unbound bacteria, the glass slides were rinsed six times with PBS in excess and sealed in Entellan (Merck) with a cover slide for fluorescence microscopy.

Quantification of Hp ex vivo binding on mouse and Mongolian gerbil gastric sections. To quantify the *ex vivo* binding of *Hp* to gastric tissue, the area of red fluorescence was measured and normalized to the whole tissue size. In brief, images were taken on an Olympus microscope with ×10 magnification and saved as multipage-TIFF files (DAPI and Cy3 channel). For analysis of *Hp ex vivo* binding, images were blinded and evaluated with ImageJ (version 1.50e). All images were calibrated (width, 1,376 pixels; height, 1,032 pixels; 1.55 pixels per µm) and analysed individually. The size of the tissue was measured by applying the free-hand selection tool on the DAPI channel and subsequently measuring the selected area (in $µm^2$). The selection was applied to the Cy3 channel and the picture was cropped accordingly. A binary image was generated using the ImageJ Threshold tool. The threshold was set individually for each picture to compensate for individual background fluorescence. The area within the binary image corresponds to the red fluorescent *Hp* bound to the tissue. The size of this area was measured in $µm^2$ and the ratio between the area of red fluorescence (Cy3 channel) and the whole tissue size was calculated and considered as the degree of *Hp ex vivo* binding to tissue samples.

Human biopsy samples. Patients who underwent upper gastrointestinal endoscopy from August 2010 to December 2013 were enrolled in the study in Nigeria, which was supported by the Africa Infectiology Initiative of the Deutsche Forschungsgemeinschaft (DFG). Upper gastrointestinal endoscopy was performed in Lagos State University Teaching Hospital, Ikeja, University College Hospital, Ibadan, Obafemi Awolowo University Teaching Hospitals Complex, Ile-Ife, Jos University Teaching Hospital, Jos, and Lagos State University Teaching Hospital, Campus Idi-Araba, Lagos. Endoscopies were performed for medically indicated reasons, not for research only. Written informed consent was obtained from each patient before enrolment, in agreement with the Helsinki Declaration. The study was reviewed and approved by an Ethics Committee of the Nigerian Institute of Medical Research (IORG0002656) and of the Ludwig-Maximilians-Universität München (registration no. 335-08). During endoscopic examination of the patients, two biopsy specimens were obtained from the gastric antrum and two from the gastric corpus. One of the samples was used for isolation of bacteria, and the other specimen was fixed in 4% formalin and embedded in paraffin for histopathological examination. *Hp* status was assessed by C14-urease test, bacterial culture and rapid urease test (CLO test) (Tri-Med Distributors). Histology with H&E staining was performed to determine pathological changes such as inflammation, metaplasia and dysplasia. Patients were considered positive for *Hp* infection when at least one of these examinations yielded positive results. Patients were defined as *Hp*-negative if all test results were negative.

Statistics. The results of image analyses were transferred to GraphPad Prism5 (GraphPad Software) to determine the statistical significance with appropriate tests. In *in vitro* experiments, to determine if the samples were normally distributed, the Shapiro–Wilk test was performed as a pre-test (≥3 independent, biological replicates) and statistical significance was assessed by the one- or two-sided Student's *t*-test. For more than two groups a one-way analysis of variance (ANOVA) was performed. In *in vivo* experiments, data that were not normally distributed were analysed by the Mann–Whitney *U*-test for unpaired groups. For the contingency tables the chi-square test was used. The size of the animal group (n) in all experiments was ≥9. The calculation of the size was based on a standard deviation (δ/σ) of 1.25, power of 80% and one-tailed Student's *t*-test. (δ = biological relative difference, σ = estimate of variation, s.e.m. = s.d./$\sqrt{n}$). Animal group sizes were as low as possible and empirically chosen. The criteria for the exclusion of animals were pre-established. No animals were excluded from any analysis. Randomization was done by a non-involved person (animal care keeper) and blinding was performed during the experiment and when assessing the outcome. Quantitative data are depicted as mean ± s.e.m. Results were considered statistically significant if the P value was below 0.05.

Data availability. The data that support the findings of this study are available from the corresponding author upon reasonable request; see author contributions for specific data sets.

Received 25 April 2016; accepted 31 August 2016; published 17 October 2016; corrected 31 October 2016

References

1. Suerbaum, S. & Michetti, P. *Helicobacter pylori* infection. *N. Engl. J. Med.* **347,** 1175–1186 (2002).
2. Peek, R. M. & Blaser, M. J. *Helicobacter pylori* and gastrointestinal tract adenocarcinomas. *Nat. Rev. Cancer* **2,** 28–37 (2002).
3. Kwok, T. *et al. Helicobacter* exploits integrin for type IV secretion and kinase activation. *Nature* **449,** 862–866 (2007).
4. Jimenez-Soto, L. F. *et al. Helicobacter pylori* type IV secretion apparatus exploits beta1 integrin in a novel RGD-independent manner. *PLoS Pathog.* **5,** e1000684 (2009).
5. Odenbreit, S. *et al.* Translocation of *Helicobacter pylori* CagA into gastric epithelial cells by type IV secretion. *Science* **287,** 1497–1500 (2000).
6. Fischer, W. *et al.* Systematic mutagenesis of the *Helicobacter pylori cag* pathogenicity island: essential genes for CagA translocation in host cells and induction of interleukin-8. *Mol. Microbiol.* **42,** 1337–1348 (2001).

7. Gorrell, R. J. *et al.* A novel NOD1- and CagA-independent pathway of interleukin-8 induction mediated by the *Helicobacter pylori* type IV secretion system. *Cell. Microbiol.* **15,** 554–570 (2013).
8. Selbach, M. *et al.* Host cell interactome of tyrosine-phosphorylated bacterial proteins. *Cell Host. Microbe* **5,** 397–403 (2009).
9. Higashi, H. *et al.* SHP-2 tyrosine phosphatase as an intracellular target of *Helicobacter pylori* CagA protein. *Science* **295,** 683–686 (2002).
10. Tsutsumi, R., Higashi, H., Higuchi, M., Okada, M. & Hatakeyama, M. Attenuation of *Helicobacter pylori* CagA-SHP-2 signaling by interaction between CagA and C-terminal Src kinase. *J. Biol. Chem.* **278,** 3664–3670 (2002).
11. Amieva, M. R. *et al.* Disruption of the epithelial apical-junctional complex by *Helicobacter pylori* CagA. *Science* **300,** 1430–1434 (2003).
12. Saadat, I. *et al. Helicobacter pylori* CagA targets PAR1/MARK kinase to disrupt epithelial cell polarity. *Nature* **447,** 330–333 (2007).
13. Ohnishi, N. *et al.* Transgenic expression of *Helicobacter pylori* CagA induces gastrointestinal and hematopoietic neoplasms in mouse. *Proc. Natl Acad. Sci. USA* **105,** 1003–1008 (2008).
14. Rieder, G., Merchant, J. L. & Haas, R. *Helicobacter pylori cag*-type IV secretion system facilitates corpus colonization to induce precancerous conditions in Mongolian gerbils. *Gastroenterology* **128,** 1229–1242 (2005).
15. Franco, A. T. *et al.* Regulation of gastric carcinogenesis by *Helicobacter pylori* virulence factors. *Cancer Res.* **68,** 379–387 (2008).
16. Hatakeyama, M. Oncogenic mechanisms of the *Helicobacter pylori* CagA protein. *Nat. Rev. Cancer* **4,** 688–694 (2004).
17. Ishijima, N. *et al.* BabA-mediated adherence is a potentiator of the *Helicobacter pylori* Type IV secretion system activity. *J. Biol. Chem.* **286,** 25256–25264 (2011).
18. Belogolova, E. *et al. Helicobacter pylori* outer membrane protein HopQ identified as a novel T4SS-associated virulence factor. *Cell. Microbiol.* **15,** 1896–1912 (2013).
19. Jimenez-Soto, L. F., Clausen, S., Sprenger, A., Ertl, C. & Haas, R. Dynamics of the Cag-type IV secretion system of *Helicobacter pylori* as studied by bacterial co-infections. *Cell Microbiol.* **15,** 1924–1937 (2013).
20. Kuespert, K., Pils, S. & Hauck, C. R. CEACAMs: their role in physiology and pathophysiology. *Curr. Opin. Cell Biol.* **18,** 565–571 (2006).
21. Gray-Owen, S. D. & Blumberg, R. S. CEACAM1: contact-dependent control of immunity. *Nat. Rev. Immunol.* **6,** 433–446 (2006).
22. Buntru, A., Roth, A., Nyffenegger-Jann, N. J. & Hauck, C. R. HemITAM signaling by CEACAM3, a human granulocyte receptor recognizing bacterial pathogens. *Arch. Biochem. Biophys.* **524,** 77–83 (2012).
23. Hauck, C. R., Agerer, F., Muenzner, P. & Schmitter, T. Cellular adhesion molecules as targets for bacterial infection. *Eur. J. Cell Biol.* **85,** 235–242 (2006).
24. Kuespert, K., Weibel, S. & Hauck, C. R. Profiling of bacterial adhesin—host receptor recognition by soluble immunoglobulin superfamily domains. *J. Microbiol. Methods* **68,** 478–485 (2007).
25. Heuermann, D. & Haas, R. A stable shuttle vector system for efficient genetic complementation of *Helicobacter pylori* strains by transformation and conjugation. *Mol. Gen. Genet.* **257,** 519–528 (1998).
26. Cao, P. & Cover, T. L. Two different families of *hopQ* alleles in *Helicobacter pylori*. *J. Clin. Microbiol.* **40,** 4504–4511 (2002).
27. Korotkova, N. *et al.* Binding of Dr adhesins of *Escherichia coli* to carcinoembryonic antigen triggers receptor dissociation. *Mol. Microbiol.* **67,** 420–434 (2008).
28. Garhart, C. A., Redline, R. W., Nedrud, J. G. & Czinn, S. J. Clearance of *Helicobacter pylori* infection and resolution of postimmunization gastritis in a kinetic study of prophylactically immunized mice. *Infect. Immun.* **70,** 3529–3538 (2002).
29. Kammerer, R. & Zimmermann, W. Coevolution of activating and inhibitory receptors within mammalian carcinoembryonic antigen families. *BMC Biol.* **8,** 12 (2010).
30. Muenzner, P., Bachmann, V., Zimmermann, W., Hentschel, J. & Hauck, C. R. Human-restricted bacterial pathogens block shedding of epithelial cells by stimulating integrin activation. *Science* **329,** 1197–1201 (2010).
31. Barrozo, R. M. *et al.* Functional plasticity in the type IV secretion system of *Helicobacter pylori*. *PLoS Pathog.* **9,** e1003189 (2013).
32. Linz, B. *et al.* An African origin for the intimate association between humans and *Helicobacter pylori*. *Nature* **445,** 915–918 (2007).
33. Schmitter, T., Agerer, F., Peterson, L., Munzner, P. & Hauck, C. R. Granulocyte CEACAM3 is a phagocytic receptor of the innate immune system that mediates recognition and elimination of human-specific pathogens. *J. Exp. Med.* **199,** 35–46 (2004).
34. Dailidiene, D., Dailide, G., Kersulyte, D., & Berg, D. E. Contraselectable streptomycin susceptibility determinant for genetic manipulation and analysis of *Helicobacter pylori*. *Appl. Environ. Microbiol.* **72,** 5908–5914 (2006).
35. Pham, K. T. *et al.* Cagi is an essential component of the *Helicobacter pylori* Cag type IV secretion system and forms a complex with CagL. *PLoS ONE* **7,** e35341 (2012).
36. Voges, M., Bachmann, V., Kammerer, R., Gophna, U. & Hauck, C. R. CEACAM1 recognition by bacterial pathogens is species-specific. *BMC Microbiol.* **10,** 117 (2010).
37. Pelegrin, A. *et al.* Human carcinoembryonic antigen cDNA expressed in rat carcinoma cells can function as target antigen for tumor localization of antibodies in nude rats and as rejection antigen in syngeneic rats. *Int. J. Cancer* **52,** 110–119 (1992).
38. Fischer, W. & Haas, R. The RecA protein of *Helicobacter pylori* requires a posttranslational modification for full activity. *J. Bacteriol.* **186,** 777–784 (2004).
39. Hohlfeld, S. *et al.* A C-terminal translocation signal is necessary, but not sufficient for type IV secretion of the *Helicobacter pylori* CagA protein. *Mol. Microbiol.* **59,** 1624–1637 (2006).
40. Odenbreit, S., Faller, G. & Haas, R. Role of the alpAB proteins and lipopolysaccharide in adhesion of *Helicobacter pylori* to human gastric tissue. *Int. J. Med. Microbiol.* **292,** 247–256 (2002).

Acknowledgements

The authors acknowledge support from collaborating gastroenterologists who collected gastric biopsies in the framework of the Africa Infectiology Study in Nigeria, especially at Lagos University Teaching Hospital, the University College Hospital (UCH) Ibadan and the University Teaching Hospital Complex Ile-Ife. The authors thank V. Naegele for CEACAM1 and CEACAM5 transfected HEK293 cells, E. Vetter for staining of CEA immunohistology sections, M. Schiemann and L. Henkel for FACS sorting of transfected cells and E. Weiss for technical support. This work was supported by grants from DFG (HA2856/6-2 to C.R.H. and HA2697/16-1, 17-1 and 18-1 and SFB914 Project B05 to R.H.) and in part by an Alexander von Humboldt Foundation Experienced Research Fellowship (to E.J.S.).

Author contributions

V.K. carried out *Hp* mutant generation, pulldown assays and knockdowns. L.H. performed mutant CEACAM construction and *Hp* binding assays. E.L. carried out microscopy studies with patient material and B.B. carried out microscopy studies with *Hp*-infected cell lines. D.A.B. investigated the expression of HopQ and CEA-N in *E. coli* and carried out ITC experiments. U.H. performed *in vivo* studies and histological experiments. A.R. generated the soluble CEACAM construct. A.K.-T. prepared and purified soluble CEACAM constructs. S.I.S. coordinated biopsies in Lagos. S.M. generated pathology data. E.J.S. analysed the ITC experimental results. W.Z. carried out CEACAM plasmid construction. Q.Z. conducted CEACAM5 luciferase reporter assays. W.F. carried out *Hp* omp gene analysis and *Hp* mutant construction. C.R.H. provided CEACAM reagents and CEA-transgenic mice. R.H. designed and coordinated the project and wrote the paper.

Additional information

Supplementary information is available for this paper.

Reprints and permissions information is available at www.nature.com/reprints.

Correspondence and requests for materials should be addressed to R.H.

How to cite this article: Königer, V. *et al. Helicobacter pylori* exploits human CEACAMs via HopQ for adherence and translocation of CagA. *Nat. Microbiol.* **2,** 16188 (2016).

Competing interests

The authors declare no competing financial interests.

Erratum: *Helicobacter pylori* exploits human CEACAMs via HopQ for adherence and translocation of CagA

Verena Königer, Lea Holsten, Ute Harrison, Benjamin Busch, Eva Loell, Qing Zhao, Daniel A. Bonsor, Alexandra Roth, Arnaud Kengmo-Tchoupa, Stella I. Smith, Susanna Mueller, Eric J. Sundberg, Wolfgang Zimmermann, Wolfgang Fischer, Christof R. Hauck and Rainer Haas

Nature Microbiology **2,** 16188 (2016); published 17 October 2016; corrected 31 October 2016.

The original version of this Article contained numerous errors in the affiliations, which were introduced during production. These have been corrected in all versions of the Article. We apologise to the authors and our readers for any confusion caused.